Effect of Solar Terms to the θ_{23} Determination in Super-Kamiokande and Important Systematic Errors for Future Improvements

Shoei NAKAYAMA
Research Center for Cosmic Neutrinos, Institute for Cosmic Ray Research, University of Tokyo, 5-1-5 Kashiwa-no-Ha, Kashiwa City, Chiba 277-8582, Japan
for the Super-Kamiokande Collaboration

Abstract

According to the LMA-MSW oscillation parameters obtained by solar neutrino experiments and the KamLAND experiment, the oscillation of low energy atmospheric ν_es might be observable even in the case of $\theta_{13} = 0$. In this paper, we will show the result of the θ_{23} determination with the Super-Kamiokande-I atmospheric neutrino data taking into account the effect of sub-dominant oscillations driven by the solar neutrino parameters. We have also researched which systematic errors should be reduced for the future determination of the octant of θ_{23} by assuming a 20 year exposure of Super-Kamiokande.

1. Introduction

The existing atmospheric neutrino data are explained very well by the pure $\nu_\mu \leftrightarrow \nu_\tau$ two flavor oscillation scheme [1]. The 2–3 oscillation parameters obtained by atmospheric neutrino observations,

$$\Delta m^2_{23} = (1.5 - 3.4) \times 10^{-3}\ \mathrm{eV}^2 \quad \text{and} \quad \sin^2 2\theta_{23} > 0.92 \quad (90\,\%\ \text{C.L.})\ [1], \tag{1}$$

have been confirmed by the long-baseline experiment using an artificial muon neutrino beam [2]. On the other hand, there is no evidence for the oscillation of atmospheric ν_e. As for the 1–3 mixing parameter, only the upper limit of $\sin^2\theta_{13}$ has been obtained by the CHOOZ reactor neutrino experiment [3]. The three flavor oscillation analysis of the Super-Kamiokande-I atmospheric neutrino data with the one mass scale dominance approximation ($\Delta m^2_{12} \sim 0$) gives the result consistent with zero $\sin^2\theta_{13}$ [4].

Recently, the 1–2 oscillation parameters were measured with the great precision by combining solar neutrino data and the KamLAND reactor neutrino data as follows [5]:

$$\Delta m^2_{12} = (7.4 - 8.5) \times 10^{-5}\ \mathrm{eV}^2 \quad \text{and} \quad \tan^2\theta_{12} = (0.33 - 0.50) \quad (1\sigma). \tag{2}$$

pp. 43–55

If these LMA-MSW oscillation parameters are taken into consideration, the oscillation of low energy (below 1 GeV) atmospheric ν_e s is expected to appear at some level regardless with the existence of the non-zero θ_{13} [6, 7]. As described in the next section, this sub-dominant oscillation effect on the sub-GeV samples depends not only on the size of the deviation of $\sin^2 2\theta_{23}$ from the maximal but also on the octant of θ_{23} (i.e., $\theta_{23} < 45°$ or $\theta_{23} > 45°$). Thus, the atmospheric neutrino analysis with the solar oscillation parameters has the possibility to determine the octant of θ_{23} for the non-maximal $\sin^2 2\theta_{23}$. It is a unique information which the planned long-baseline experiments and reactor experiments can not explore in the zero θ_{13} case.

2. Sub-dominant Oscillation Effect on Sub-GeV samples

We assume $\theta_{13} = 0$ for all the analyses in this paper. As widely discussed in the literature [6, 7], the relative change on the atmospheric ν_e flux due to oscillations driven by the solar neutrino parameters is written as follows:

$$\frac{F_e^{\rm osc}}{F_e^0} - 1 = P_2 \ (\ r\cos^2\theta_{23} - 1 \ ) \ , \tag{3}$$

where $F_e^{\rm osc}$ and F_e^0 are the atmospheric ν_e fluxes with and without oscillations, and $r \equiv F_\mu^0 / F_e^0$ is the ratio of the original atmospheric ν_μ and ν_e fluxes. P_2 is the two neutrino transition ($\nu_e \rightarrow \nu_x$) probability in matter driven by the 1–2 parameters. Fig. 1 shows the calculated P_2 at the Super-Kamiokande site for atmosphric neutrinos with an energy of E_ν and a direction of $\cos\Theta_\nu$. In the figure, the 1–2 oscillation parameters are assumed as $\Delta \mathrm{m}_{12}^2 = 8.3 \times 10^{-5}\,\mathrm{eV}^2$ and $\tan^2\theta_{12} = 0.41$, which are well in the allowed region Eq.(2) by the solar neutrino and KamLAND experiments. From Eq.(3) and Fig. 1, it is found that the oscillation effect is larger for lower energy ν_e s. Thus, the sub-GeV atmospheric neutrino samples play an important role for observing a sub-dominant effect driven by the solar neutrino parameters. Note that the probability P_2, and consequently the oscillation effect on the ν_e flux, increase also with $\Delta \mathrm{m}_{12}^2$.

The factor in brackets in Eq.(3) is called the "screening" factor. In fact, since the ν_μ and ν_e flux ratio $r \sim 2$ in the sub-GeV neutrino energy region [8, 9, 10], the screening factor is very small in the case of the maximal 2–3 mixing (i.e., $\theta_{23} = 45°$). According to the screening factor, the appearance of the sub-dominant oscillation effect depends largely on the deviation of $\sin^2 2\theta_{23}$ from the maximal. If θ_{23} is in the first octant, $\theta_{23} < 45°$, the screening factor is positive and an excess of the sub-GeV e-like sample is expected. If θ_{23} is in the second octant, $\theta_{23} > 45°$, the screening factor is negative and the sub-GeV e-like sample is expected to be reduced.

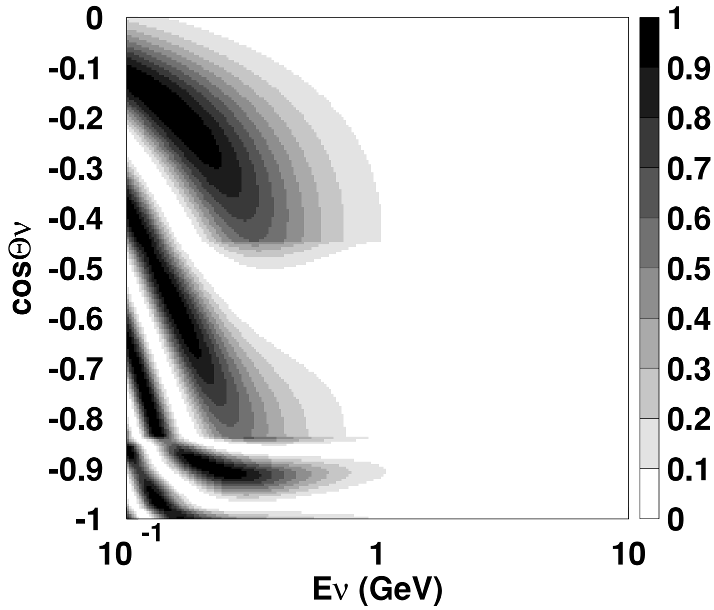

Fig 1. The calculated two neutrino transition probability P_2 at the SK site for atmosphric neutrinos with an energy of E_ν (horizontal axis) and a direction of $\cos\Theta_\nu$ (vertical axis). The Earth's matter effect is taken into account. The 1–2 oscillation parameters are assumed as $\Delta m^2_{12} = 8.3 \times 10^{-5}\,\mathrm{eV}^2$ and $\tan^2\theta_{12} = 0.41$.

In order to see the size of sub-dominant oscillation effects on the sub-GeV samples, we employ the Super-Kamiokande atmosphric neutrino Monte Carlo simulation [1, 4]. Fig. 2 shows the zenith angle dependence of relative effect due to 1–2 oscillations on the number of FC sub-GeV single-ring e-like events for different values of $\sin^2\theta_{23}$. The 1–2 oscillation parameters are assumed again as $\Delta m^2_{12} = 8.3 \times 10^{-5}\,\mathrm{eV}^2$ and $\tan^2\theta_{12} = 0.41$. In the figure, the number of e-like events with sub-dominant 1–2 oscillations (N_e^{osc}) is normalized by the number of e-like events with pure $\nu_\mu \leftrightarrow \nu_\tau$ two flavor full-mixing oscillations ($N_e^{2\,\mathrm{flavor\,full-mixing}}$). Though ν_e does not oscillate at all in the pure $\nu_\mu \leftrightarrow \nu_\tau$ two flavor oscillation scenario, $N_e^{2\,\mathrm{flavor\,full-mixing}}$ differs from N_e^0 (i.e., the number of events with no oscillation) because the FC sub-GeV single-ring e-like sample contains a few percent contamination of ν_μCC interactions. As seen in Fig. 2, the sub-dominant oscillation effect is negligible for $\sin^2\theta_{23} = 0.5$ (solid line). For $\sin^2\theta_{23} = 0.4$ (dashed line) and 0.6 (dotted line), the sub-dominant effect appears as a $1 \sim 2\,\%$ excess and deficiency of sub-GeV e-like events, respectively. It is found that the estimated size of the effect is smaller than the statistical error of existing Super-Kamiokande data, about $5\,\%$. Fig. 3 shows again the zenith angle dependence of relative effect due to 1–2 oscillations for two sub-samples of the

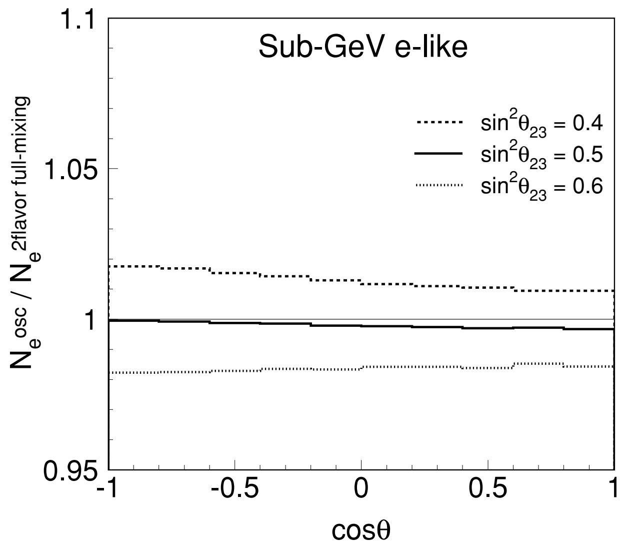

Fig 2. Zenith angle dependence of the ratio of the number of FC sub-GeV single-ring e-like events including sub-dominant oscillations due to the solar neutrino parameters ($N_e^{\rm osc}$) and the number of FC sub-GeV single-ring e-like events with pure $\nu_\mu \leftrightarrow \nu_\tau$ two flavor full-mixing oscillations ($N_e^{2\,\rm flavor\,full-mixing}$). For calculation of $N_e^{\rm osc}$, $\Delta m^2_{12} = 8.3\times10^{-5}\,{\rm eV}^2$, $\tan^2\theta_{12} = 0.41$, $\Delta m^2_{23} = 2.5\times10^{-3}\,{\rm eV}^2$ and 3 different θ_{23} s, $\sin^2\theta_{23} = 0.4$ (dashed line), 0.5 (solid line) and 0.6 (dotted line) are assumed. For calculation of $N_e^{2\,\rm flavor\,full-mixing}$, $\Delta m^2_{23} = 2.5\times10^{-3}\,{\rm eV}^2$ and $\sin^2\theta_{23} = 0.5$ are assumed.

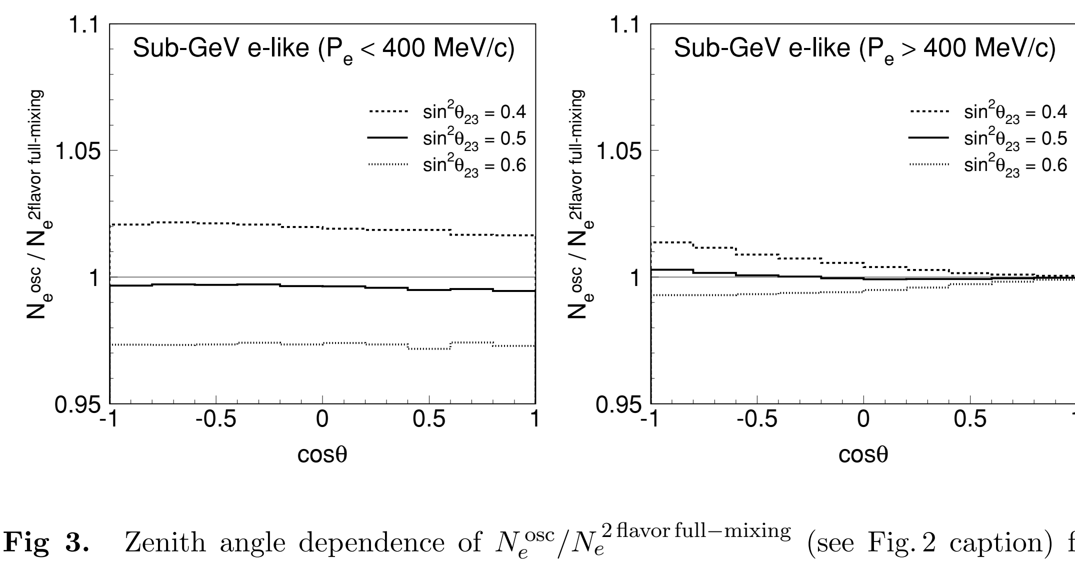

Fig 3. Zenith angle dependence of $N_e^{\rm osc}/N_e^{2\,\rm flavor\,full-mixing}$ (see Fig. 2 caption) for sub-samples of the FC sub-GeV single-ring e-like sample with electron momentum below 400 MeV/c (left) and that with electron momentum above 400 MeV/c (right). The difference in line types is described in Fig. 2 caption.

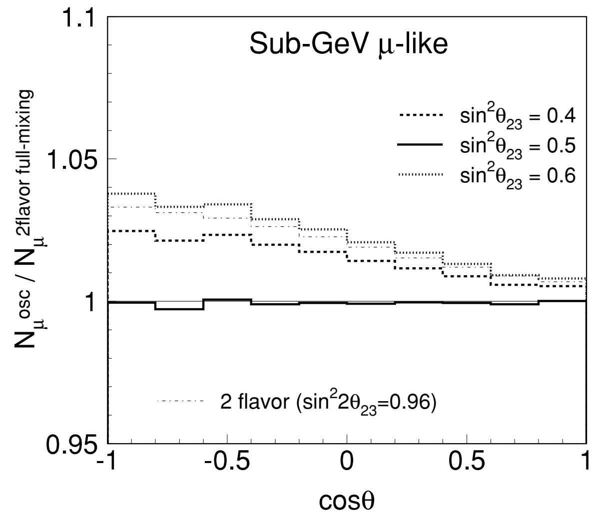

Fig 4. Zenith angle dependence of the ratio of the number of FC sub-GeV single-ring μ-like events including sub-dominant oscillations due to the solar neutrino parameters ($N_\mu^{\rm osc}$) and the number of FC sub-GeV single-ring μ-like events with pure $\nu_\mu \leftrightarrow \nu_\tau$ two flavor full-mixing oscillations ($N_\mu^{\rm 2\,flavor\,full-mixing}$). For thick lines, $\Delta{\rm m}^2_{12} = 8.3 \times 10^{-5}\,{\rm eV}^2$, $\tan^2\theta_{12} = 0.41$, $\Delta{\rm m}^2_{23} = 2.5 \times 10^{-3}\,{\rm eV}^2$, $\sin^2\theta_{23} = 0.4$ (dashed line), 0.5 (solid line) and 0.6 (dotted line) are assumed to calculate $N_\mu^{\rm osc}$. For a dash-dotted thin line, the numerator is the number of μ-like events in the case of pure $\nu_\mu \leftrightarrow \nu_\tau$ two flavor oscillations with $\sin^2 2\theta_{23} = 0.96$, which corresponds to $\sin^2\theta_{23} = 0.4$ or $\sin^2\theta_{23} = 0.6$.

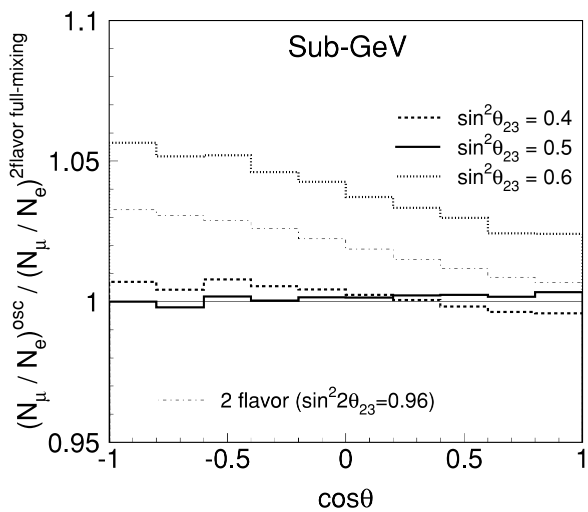

Fig 5. Zenith angle dependence of the N_μ/N_e ratio including sub-dominant oscillations due to the solar neutrino parameters normalized by the N_μ/N_e ratio with pure $\nu_\mu \leftrightarrow \nu_\tau$ two flavor full-mixing oscillations. The difference in line types is described in Fig. 4 caption.

FC sub-GeV single-ring e-like sample divided by the reconstructed electron momentum. As expected from Fig. 1, the effect is larger for the sub-sample made by atmospheric neutrinos with lower energies. In the higher energy sub-sample in Fig. 3, the size of the effect is smaller but its zenith angle dependence is stronger. This is because the direction of a higher momentum lepton has stronger correlation to the parent neutrino direction.

The sub-dominant oscillation effect due to the solar neutrino parameters appears also on the sub-GeV μ-like sample as shown in Fig. 4. The relative effect is found to be very small for $\sin^2\theta_{23} = 0.5$ (solid line). Since the number of FC sub-GeV single-ring μ-like events is modified largely by the dominant oscillation channel $\nu_\mu \leftrightarrow \nu_\tau$, the relative effect of sub-dominant oscillations for $\sin^2\theta_{23} = 0.4$ (dashed line) and 0.6 (dotted line) can be extracted by compared with the case of pure two flavor oscillations with the corresponding $\sin^2 2\theta_{23}$, namely 0.96 (dash-dotted thin line). By comparing the dashed and dotted thick lines with the dash-dotted thin line in Fig. 4, one can find that the direction of the sub-dominant oscillation effect (i.e., an excess or a deficiency) on the μ-like sample is opposite to that on the e-like sample. Therefore, the discrimination between $\sin^2\theta_{23} = 0.4$ and $\sin^2\theta_{23} = 0.6$ is expected to be larger by taking the μ/e ratio. Fig. 5 shows the zenith angle dependence of the sub-dominant 1–2 oscillation effect on the ratio between the number of FC sub-GeV single-ring μ-like events and the number of FC sub-GeV single-ring e-like events. In the upward vertical bin, the difference on the μ/e ratio between for the $\sin^2\theta_{23} = 0.4$ case and for the $\sin^2\theta_{23} = 0.6$ case reach about 5 %, which is comparable to the size of the estimated systematic error on the μ/e ratio [1].

Thus, an oscillation analysis of the sub-GeV samples taking into account the sub-dominant 1–2 oscillation has the possibility to determine the octant of θ_{23} for the non-maximal $\sin^2 2\theta_{23}$. Of course, the deviation of $\sin^2 2\theta_{23}$ affects other observables, especially the zenith angle dependence of μ-like events. Therefore in order to determine $\sin^2\theta_{23}$, we need a combined oscillation analysis of all the samples with systematic errors properly estimated.

3. Oscillation Analysis with the Solar Neutrino Parameters using the Super-Kamiokande-I Atmospheric Neutrino Data

In this section, we present the result of a $\sin^2\theta_{23}$ measurement using the atmospheric neutrino data from a 1489 day exposure of the Super-Kamiokande detector. The fully-contained, partially-contained, and upward-going muon data are compared with expectations by a 100 years equivalent detailed Monte Carlo simulation including atmospheric neutrino flux calculations, neutrino interactions, and

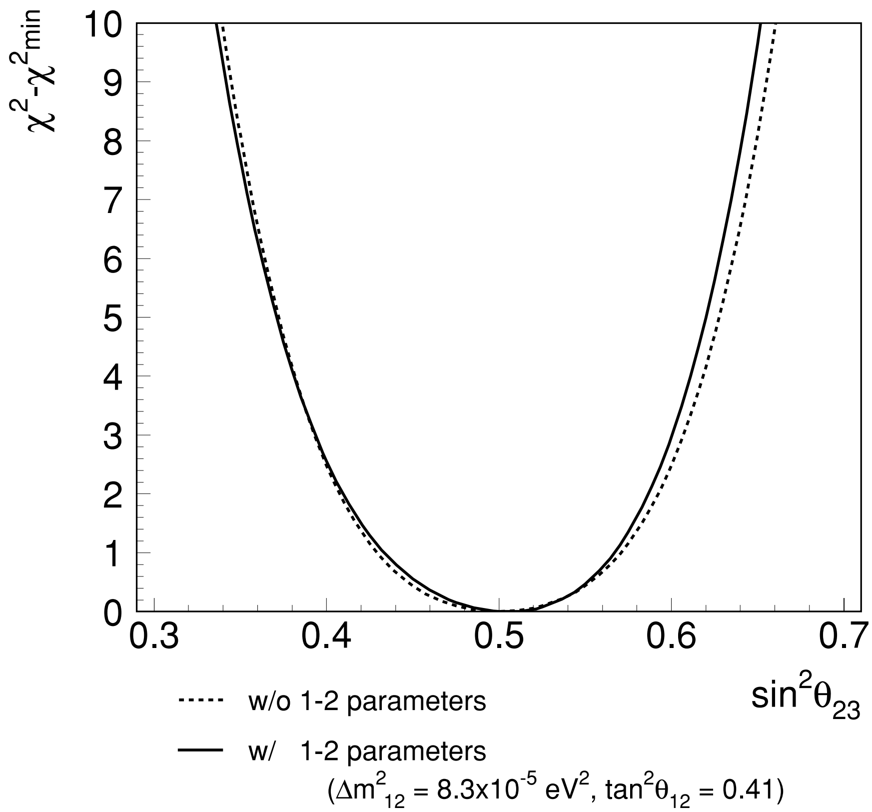

Fig 6. The $\chi^2 - \chi^2_{\rm min}$ distribution as a function of $\sin^2\theta_{23}$ for oscillations without the 1–2 parameters (dashed line) and with the 1–2 parameters (solid line) by the atmospheric neutrino data from a 1489 day exposure of the Super-Kamiokande detector. $\theta_{13} = 0$ is assumed. In the case with the 1–2 parameters, $\Delta m^2_{12} = 8.3 \times 10^{-5}\,\rm eV^2$ and $\tan^2\theta_{12} = 0.41$ are assumed. For each $\sin^2\theta_{23}$ point, Δm^2_{23} is chosen so that χ^2 is minimized.

detector performances. A detailed description of our oscillation analysis method (i.e., the number of data bins, the oscillation probability calculation, the definition and minimization of χ^2, the systematic errors, etc.) can be found in Ref. [4].

As previously mentioned, $\theta_{13} = 0$ is assumed in this analysis. For the solar neutrino parameters, we examine two scenarios. In the scenario with the solar neutrino parameters turned on, $\Delta m^2_{12} = 8.3 \times 10^{-5}\,\rm eV^2$ and $\tan^2\theta_{12} = 0.41$ are chosen. The other scenario is ordinary "one mass scale dominance" approximation with $\Delta m^2_{12} = 0$, that is, pure $\nu_\mu \leftrightarrow \nu_\tau$ two flavor oscillation scenario. Since three oscillation parameters (θ_{13}, θ_{12} and Δm^2_{12}) are fixed, χ^2 is calculated in the two dimensional oscillation parameter space of Δm^2_{23} and $\sin^2\theta_{23}$.

Fig. 6 shows the $\sin^2\theta_{23}$ dependence of the $\chi^2 - \chi^2_{\rm min}$ function marginalized with respect to Δm^2_{23}, for two scenarios with and without the solar neutrino parameters. It is found that the best-fit point is located at $\sin^2\theta_{23} = 0.5$ in both

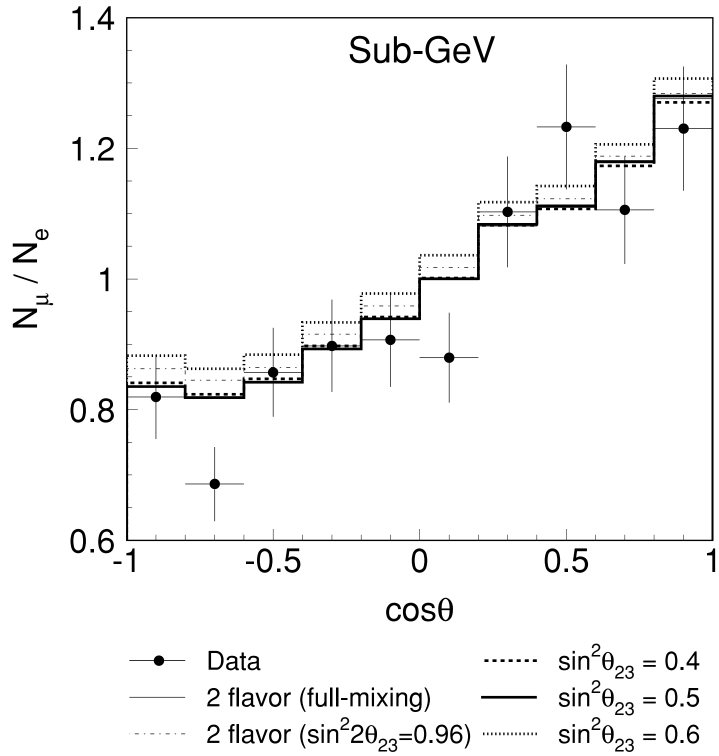

Fig 7. Zenith angle dependence of the ratio between the number of FC sub-GeV single-ring μ-like events and the number of FC sub-GeV single-ring e-like events, for observed data (dots), Monte Carlo expectations with pure $\nu_\mu \leftrightarrow \nu_\tau$ oscillations (thin lines) and Monte Carlo expectations with sub-dominant oscillations (thick lines).

cases. Though the difference in the χ^2 distribution between two scenarios is rather small, one can find that, in the large $\sin^2\theta_{23}$ region, χ^2 with the sub-dominant oscillation is larger than that with pure $\nu_\mu \leftrightarrow \nu_\tau$ oscillations. The reason can roughly be understood by looking at the μ/e ratio distribution. Fig. 7 shows the zenith angle dependence of the ratio between the number of FC sub-GeV single-ring μ-like events and the number of FC sub-GeV single-ring e-like events. It is found that this sample prefer $\sin^2\theta_{23} = 0.4$ or $\sin^2\theta_{23} = 0.5$ to $\sin^2\theta_{23} = 0.6$.

Recently, several groups have done similar analyses using the SK data and got results with the best-fit point located at $\sin^2\theta_{23}$ below 0.5 [11, 12, 13], which is easily expected from the fact that some excess of sub-GeV e-like events exists. The largest difference between our analysis method and theirs is the sample division. In our χ^2 calculation, the sub-GeV sample is divided into sub-samples by reconstructed lepton momenta. That might be the reason for the difference in the best-fit $\sin^2\theta_{23}$. A careful study will be needed on this issue.

4. Future Sensitivities on the $\boldsymbol{\theta}_{23}$ Determination and Important Systematic Errors

The future sensitivity on the θ_{23} determination can be researched by simulating the signal according to the expectation from some specific choice of the true oscillation parameters. We utilize, instead of the observed data, the oscillated Monte Carlo sample reweighted to a 20 year exposure of the Super-Kamiokande detector, about 4 times the whole Super-Kamiokande-I data. Four different values, 0.40, 0.45, 0.55 and 0.60, are selected as the true $\sin^2\theta_{23}$. As for the other parameters, $\theta_{13} = 0$, $\tan^2\theta_{12} = 0.41$, $\Delta m^2_{12} = 8.3 \times 10^{-5}\,\mathrm{eV}^2$ and $\Delta m^2_{23} = 2.5 \times 10^{-3}\,\mathrm{eV}^2$ are assumed both for making the fake signal and for the expectation to calculate χ^2. Therefore, we search only $\sin^2\theta_{23}$ for the χ^2 minimum. A total of 44 systematic error parameters, which represent the uncertainties of sample normalizations, neutrino flux calculations, neutrino interaction models and detector responses, are considered in our Monte Carlo expectation. A list of our systematic error estimations can be found elsewhere [1, 4]. In this study, to research which systematic errors should be reduced for getting a better sensitivity, the size of specific systematic errors is reduced down to 1/4 of the current estimation and then χ^2 distributions are compared.

Fig. 8 shows the $\sin^2\theta_{23}$ dependence of $\chi^2 - \chi^2_{\mathrm{min}}$ for each true $\sin^2\theta_{23}$. A solid thick line in each figure is for the case with all the systematic errors unchanged. We see that the best-fit point is located at the true $\sin^2\theta_{23}$ value, while in the true $\sin^2\theta_{23} = 0.40$ case (top left) and 0.60 case (bottom right) the χ^2 distribution has a second local minimum around the false answer $1 - \sin^2\theta_{23}$. It seems to be difficult to measure $\sin^2\theta_{23}$ precisely in this statistics in the case that the deviation of $\sin^2 2\theta_{23}$ from the maximal is small. In Fig. 8, the other lines are for cases where we reduce the systematic errors in atmospheric neutrino flux (dashed line), neutrino interaction (dotted line), event selection and event reconstruction (dash-dotted line), and all the systematic errors (solid thin line). One can find that reducing the neutrino interaction systematic errors is most important to distinguish the true answer from the false one.

To look more closely, χ^2 distributions are compared by reducing each systematic error parameter among 44 parameters one by one. Though we can not present each χ^2 distribution due to limited space, we see that dominant systematic errors to be reduced for the future determination of $\sin^2\theta_{23}$ are as follows:

(a) neutrino flux : $(\nu_\mu + \overline{\nu}_\mu)\,/\,(\nu_e + \overline{\nu}_e)$ for $E_\nu < 5\,\mathrm{GeV}$

> 3 % error is currently assigned by comparing three atmospheric neutrino flux calculations in Refs. [8], [9] and [10].

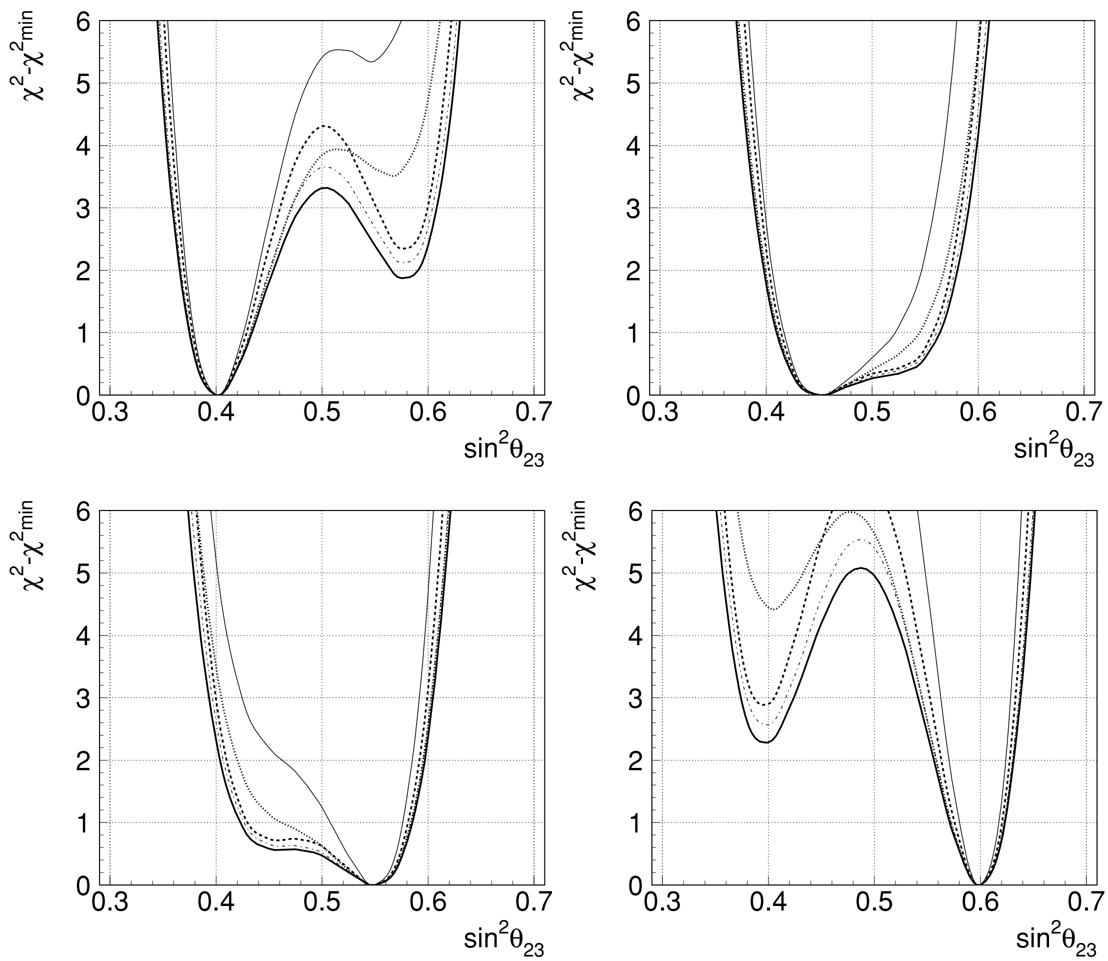

Fig 8. The $\chi^2 - \chi^2_{\rm min}$ distribution as a function of $\sin^2\theta_{23}$ using the oscillated Monte Carlo simulation for a 20 year exposure of SK with the true oscillation parameters of $\theta_{13} = 0$, $\tan^2\theta_{12} = 0.41$, $\Delta m^2_{12} = 8.3 \times 10^{-5}\,{\rm eV}^2$, $\Delta m^2_{23} = 2.5 \times 10^{-3}\,{\rm eV}^2$, and $\sin^2\theta_{23} = 0.40$ (top left), 0.45 (top right), 0.55 (bottom left), 0.60 (bottom right). The difference in line types represents a choice of the systematic error estimation (see text).

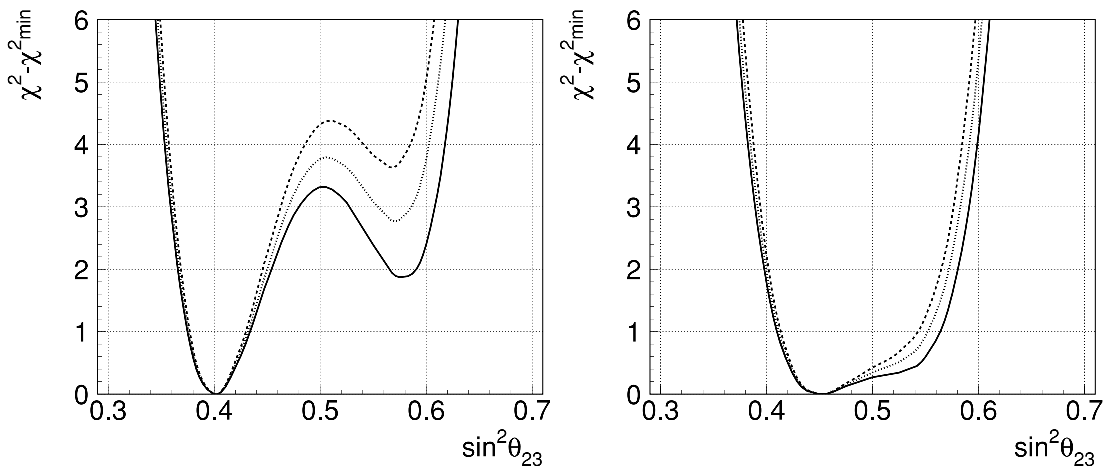

Fig 9. The $\chi^2 - \chi^2_{\rm min}$ distribution as a function of $\sin^2\theta_{23}$ using the oscillated Monte Carlo simulation for a 20 year exposure of SK with the true $\sin^2\theta_{23}$ of 0.40 (left) and 0.45 (right). The size of the 7 dominant systematic errors is assumed as 1/2 (dotted line) and 1/4 (dashed line) of the current estimation.

(b) neutrino flux : $\nu_e \,/\, \overline{\nu}_e$ for $E_\nu < 10\,\mathrm{GeV}$

5 % error is currently assigned by comparing three atmospheric neutrino flux calculations in Refs. [8], [9] and [10].

(c) neutrino flux : $\nu_\mu \,/\, \overline{\nu}_\mu$ for $E_\nu < 10\,\mathrm{GeV}$

5 % error is currently assigned by comparing three atmospheric neutrino flux calculations in Refs. [8], [9] and [10].

(d) neutrino flux : up/down

0.5 %, 0.8 %, 2.1 %, and 1.8 % errors are currently assigned for
the FC sub-GeV single-ring e-like sample with $P_e < 400\,\mathrm{MeV}/c$,
the FC sub-GeV single-ring μ-like sample with $P_\mu < 400\,\mathrm{MeV}/c$,
the FC sub-GeV single-ring e-like sample with $P_e > 400\,\mathrm{MeV}/c$, and
the FC sub-GeV single-ring μ-like sample with $P_\mu > 400\,\mathrm{MeV}/c$, respectively.

(e) neutrino interaction : M_A in quasi-elastic scattering and single-π production

10 % uncertainty is currently assigned to the axial vector mass, M_A, which is set to $1.1\,\mathrm{GeV}/c^2$.

(f) neutrino interaction : nuclear effects in quasi-elastic cross section calculation

The difference between the model in Ref. [1, 14] and the model in Ref. [15] is adopted as a systematic error.

(g) neutrino interaction : NC/CC cross section ratio

20 % error is currently assigned.

Fig. 9 shows the $\sin^2\theta_{23}$ dependence of $\chi^2 - \chi^2_{\rm min}$ for two true $\sin^2\theta_{23}$ points, 0.40 (left) and 0.45 (right), with these 7 dominant systematic errors reduced simultaneously down to 1/2 (dotted line) and 1/4 (dashed line) of current estimations.

5. Conclusions

The appearance of the sub-dominant oscillation effect on the low energy atmospheric neutrino sample due to the solar neutrino parameters depends strongly on the deviation of $\sin^2\theta_{23}$ from 0.5. The result of an oscillation analysis with the solar neutrino parameters using the Super-Kamiokande-I atmospheric neutrino data gives no change on the best-fit $\sin^2\theta_{23}$ at 0.5, while there exists small change on the χ^2 distribution shape, compared with the result of an analysis without the solar neutrino parameters. The future sensitivity on the $\sin^2\theta_{23}$ determination with the solar neutrino parameters is estimated by assuming a 20 year exposure of Super-Kamiokande. It is found that dominant systematic errors for the future improvement are uncertainties on ν_μ/ν_e , $\nu/\overline{\nu}$, and up/down flux ratios for low energy neutrinos, the quasi-elastic scattering model, and the NC/CC cross section ratio.

References

[1] Y. Ashie *et al.* [Super-Kamiokande Collaboration], arXiv:hep-ex/0501064.

[2] E. Aliu *et al.* [K2K Collaboration], Phys. Rev. Lett. **94** (2005) 081802 [arXiv:hep-ex/0411038].

[3] M. Apollonio *et al.*, Eur. Phys. J. C **27** (2003) 331 [arXiv:hep-ex/0301017].

[4] K. Okumura, "Constraint on θ_{13} from the Super-Kamiokande Atmospheric Neutrino Data", in these Proceedings.

[5] T. Araki *et al.* [KamLAND Collaboration], Phys. Rev. Lett. **94** (2005) 081801 [arXiv:hep-ex/0406035].

[6] O. L. G. Peres and A. Y. Smirnov, Phys. Lett. B **456** (1999) 204 [arXiv:hep-ph/9902312].

[7] O. L. G. Peres and A. Y. Smirnov, Nucl. Phys. B **680** (2004) 479 [arXiv:hep-ph/0309312].

[8] M. Honda, T. Kajita, K. Kasahara and S. Midorikawa, Phys. Rev. D **70** (2004) 043008 [arXiv:astro-ph/0404457].

[9] G. D. Barr, T. K. Gaisser, P. Lipari, S. Robbins and T. Stanev, Phys. Rev. D **70** (2004) 023006 [arXiv:astro-ph/0403630].

[10] G. Battistoni, A. Ferrari, T. Montaruli and P. R. Sala, arXiv:hep-ph/0305208.

[11] M. C. Gonzalez-Garcia, M. Maltoni and A. Y. Smirnov, Phys. Rev. D **70** (2004) 093005 [arXiv:hep-ph/0408170].

[12] M. C. Gonzalez-Garcia, "Sub-dominant Oscillation Effects in Atmospheric Neutrinos", in these Proceedings.

[13] E. Lisi, "Three-flavor Subleading Effects and Systematic Uncertainties in Super-Kamiokande", in these Proceedings.

[14] Y. Hayato, Nucl. Phys. Proc. Suppl. **112** (2002) 171.

[15] S. K. Singh and E. Oset, Phys. Rev. C **48** (1993) 1246.